

The phase diagram of cobalt at high pressure and temperature: the stability of  $\gamma^{(\text{fcc})}$ -cobalt and new  $\epsilon'(\text{dhcp})$ -cobalt

This article has been downloaded from IOPscience. Please scroll down to see the full text article.

1998 J. Phys.: Condens. Matter 10 L311

(<http://iopscience.iop.org/0953-8984/10/20/001>)

View [the table of contents for this issue](#), or go to the [journal homepage](#) for more

Download details:

IP Address: 171.66.16.151

The article was downloaded on 12/05/2010 at 23:22

Please note that [terms and conditions apply](#).

## LETTER TO THE EDITOR

**The phase diagram of cobalt at high pressure and temperature: the stability of  $\gamma$ (fcc)-cobalt and new  $\varepsilon'$ (dhcp)-cobalt**

Choong-Shik Yoo, Per Söderlind and Hyunhae Cynn  
Lawrence Livermore National Laboratory, Livermore, CA 94551, USA

Received 17 February 1998

**Abstract.** A metastable dhcp phase of cobalt,  $\varepsilon'$ -Co, has been discovered below 60 GPa by using *in situ* x-ray diffraction and a laser-heated diamond-anvil cell. The volume at 34 GPa is  $59.01 \text{ cm}^3 \text{ mol}^{-1}$  with  $c/a = 3.190$ . First-principles theory shows that  $\varepsilon'$ (dhcp)-Co and  $\varepsilon$ (hcp)-Co are close in energy below 60 GPa, and that temperature and magnetic effects can make dhcp-Co more stable than hcp-Co. The  $\gamma$ (fcc)-phase is found to be stable and quenchable over a wide range of pressure and temperature. New constraints for the phase diagram of Co are presented.

The crystal structures and periodic behaviour of nonmagnetic d transition elements have been known for a long time. As a function of atomic number, all nonmagnetic transition metals show the same structural behaviour, namely  $\text{hcp} \rightarrow \text{bcc} \rightarrow \text{hcp} \rightarrow \text{fcc}$  under ambient conditions [1]. This systematic change can be explained in terms of the filling of d bands whose shapes mostly depend upon the crystal structure [2, 3], and this explanation can be generalized to explain also the pressure-induced phase transitions and the crystal structures of magnetic d transition metals [4]. Hence, with the exception of that of Mn, the crystal structures of d transition metals are all simple: bcc, hcp, and fcc.

The behaviour of iron contrasts with the systematic behaviour of d-band transition metals: dhcp ( $\varepsilon'$ -Fe [5, 6] and  $\beta$ -Fe [7]) and orthorhombic ( $\beta$ -Fe [8]) phases were recently discovered in its phase diagram. These discoveries are of significance to research related to the Earth's core, but are also of fundamental interest because of the novelty of the dhcp and orthorhombic structures in the series of d transition metals. Consequently, these phases have aroused some scepticism, and their stabilities and structures have been controversial [9–11]. Cobalt, being the metal following iron in the periodic table, is potentially important as regards the properties of the Earth's core, which is believed to be composed of iron-dominated alloys with perhaps Co or Ni as minor components. Furthermore, the structural behaviour of Co at high pressure and temperature may shed light on the phase diagram of iron in general, and the  $\varepsilon'$ -Fe and  $\beta$ -Fe phases in particular. Hence, both (i) the wish to achieve a fundamental understanding of the d transition metals and (ii) the connection to the Earth's core have motivated us to investigate the phase diagram of Co by means of high-pressure and high-temperature experiments together with first-principles theoretical calculations.

Cobalt crystallizes into a ferromagnetic hcp structure,  $\varepsilon$ -Co, under ambient conditions [12, 13]. This is in contrast to the 4d and 5d counterparts Rh and Ir showing nonmagnetic fcc structure. The fact that the hcp structure is more stable than the fcc structure in Co is due

to the presence of magnetism, and this has been explained in detail [4]. Therefore, at higher pressures where the magnetism is sufficiently suppressed, we anticipate a transition from hcp to fcc structure in Co. Similarly, iron transforms from its bcc phase to its hcp phase at about 10 GPa, whereas Ni is expected to remain in the fcc phase at higher pressures.

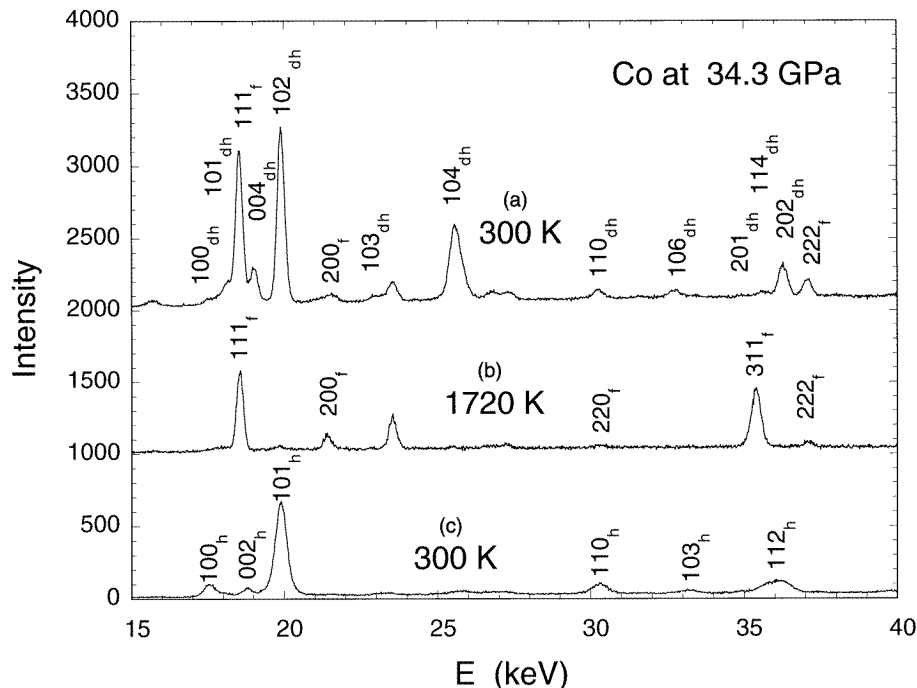


**Figure 1.** The x-ray diffraction patterns of cobalt in  $\text{Al}_2\text{O}_3$  at 34.3 GPa, (a) before (300 K), (b) during (1720 K), and (c) after heating (300 K).

The hcp phase of  $\epsilon$ -Co transforms to the fcc structure  $\gamma$ -Co at high temperatures near 700 K; this is also ferromagnetic and stable up to the melting temperatures which are near 1770 K [13]. The  $\gamma$ -phase of Co becomes paramagnetic above the Curie temperature, 1400 K, under ambient pressure. The  $\epsilon/\gamma$ -phase boundary has been found by measurement to be 100 GPa; the  $\epsilon/\gamma$ /liquid triple point was suggested to be at 3300 K at 100 GPa [14]. However, we should note that the criteria for determining the  $\epsilon/\gamma$ -phase transition in the above measurements were based on the change in laser reflectivity of a laser-heated sample [14, 15], not on the change in crystal structure. In fact, the fcc structure of  $\gamma$ -Co has not been previously observed at high pressures and temperatures.

In this letter, we report our structural investigation of Co up to 100 GPa and 3000 K, in conjunction with a first-principles (low-temperature) theory up to 200 GPa; we also present new constraints for the phase diagram of Co. Our major results include the discoveries (i) of a new metastable  $\epsilon'$ (dhcp)-Co phase below 60 GPa, and (ii), in contrast to the case for  $\gamma$ (fcc)-Fe, that  $\gamma$ (fcc)-Co is stable over a wide range of pressures above 70 GPa.

The crystal structures of cobalt at high pressures and temperatures have been investigated in a diamond-anvil cell by using the *in situ* x-ray/laser-heating technique [5, 6]. A small piece of thin, 10–12  $\mu\text{m}$ , cobalt foil is loaded into a diamond-anvil cell, together with a pressure medium such as Ar or  $\text{Al}_2\text{O}_3$ . The sample is heated by using a Nd:YAG single-

**Table 1.** The x-ray diffraction pattern of cobalt at 34.3 GPa and 300 K, quenched from 1720 K. The fitting was based on a mixture of  $\epsilon'$ (dhcp)-Co and  $\gamma$ (fcc)-Co. ( $E_d = 36.607$  keV  $\text{\AA}$ .)

$d_{\text{obs}}$	$M(hkl)$	$d_{\text{cal}}$ (dhcp)	$d_{\text{cal}}$ (fcc)	$\Delta d$
2.319				
2.094	$\epsilon'$ (100)	2.097		0.003
2.024	$\epsilon'$ (101)	2.023		-0.001
1.974	$\gamma$ (111)		1.968	-0.006
1.922	$\epsilon'$ (004)	1.930		0.008
1.838	$\epsilon'$ (102)	1.842		0.004
1.699	$\gamma$ (200)	1.704	0.005	
1.594	$\epsilon'$ (103)	1.623		-0.019
1.557				
1.430	$\epsilon'$ (104)	1.421		-0.009
1.371	$\gamma$ (211)		1.391	-0.020
1.210	$\epsilon'$ (110)	1.210		0.000
	$\gamma$ (220)		1.205	-0.005
1.116	$\epsilon'$ (106)	1.099		0.017
1.043	$\epsilon'$ (201)	1.039		-0.004
1.029	$\epsilon'$ (114)	1.026		-0.003
	$\gamma$ (311)		1.028	-0.001
1.009	$\epsilon'$ (202)	1.012		0.003
0.987	$\gamma$ (222)		0.984	-0.003

$\epsilon'$ (dhcp):  $a = 2.421$   $\text{\AA}$ ,  $c = 7.722$   $\text{\AA}$ ,  $V = 59.01$   $\text{cm}^3$   $\text{mol}^{-1}$   
 $\gamma$ (fcc):  $a = 3.408$   $\text{\AA}$ ,  $V = 59.62$   $\text{cm}^3$   $\text{mol}^{-1}$   
 $\epsilon$ (hcp)\*:  $a = 2.412$   $\text{\AA}$ ,  $c = 3.891$   $\text{\AA}$ ,  $V = 58.89$   $\text{cm}^3$   $\text{mol}^{-1}$

\* The lattice parameters for  $\epsilon$ -Co were from the fitting of trace (a) in figure 1.

sided laser-heating system, which could give rise to a large uncertainty in temperature: near 10% [5, 16]. White x-ray radiation from a synchrotron source is coaxially focused to the centre of the laser-heating spot, and the x-ray diffraction is recorded at a fixed  $2\Theta$  angle between  $19^\circ$  and  $21^\circ$  as a function of energy. The pressure of the sample is then determined either from the equation of state (EoS) of the sample or by a ruby luminescence method.

Figure 1 shows diffraction patterns of cobalt in  $\text{Al}_2\text{O}_3$  at 34.3 GPa under various conditions. The diffraction pattern of cobalt before heating, trace (a), can be easily indexed to  $\epsilon$ -Co as illustrated in the figure. At 1720 K, trace (b), the diffraction pattern changes to a new one, which can also be indexed well to  $\gamma$ -Co with  $a = 3.424$   $\text{\AA}$ ,  $V = 60.444$   $\text{cm}^3$   $\text{mol}^{-1}$ . The diffraction pattern after heating, trace (c), is, however, complicated by the appearance of several new features in addition to those arising from  $\gamma$ -Co. The 111, 200, 311, and 222 reflections are most characteristic of the fcc structure, respectively at 18.54, 21.54, 35.58, 37.10 keV, suggesting that  $\gamma$ -Co is quenchable at low temperatures at high pressures, like  $\gamma$ -Fe [5, 6]. Other features in trace (c) in figure 1 appear to be quite different from those for  $\epsilon$ -Co. For example, a quartet is evident between 17 and 20 keV in trace (c), contrasting with the triplet characteristic to  $\epsilon$ -Co evident in trace (a). Several new features also appear at 23.0, 25.6, 36.38 keV. These diffraction changes are entirely reproducible for many cycles of heating, and also occur in Ar, precluding the possibility of a chemical reaction between Co and the pressure medium.

Clearly, the quenched diffraction pattern indicates that some of the  $\gamma$ -Co transforms to a new structure. Several structures have been considered, including orthorhombic, dhcp, hcp, and a mixture of two hcp structures; the best fit of the diffraction pattern shown as trace

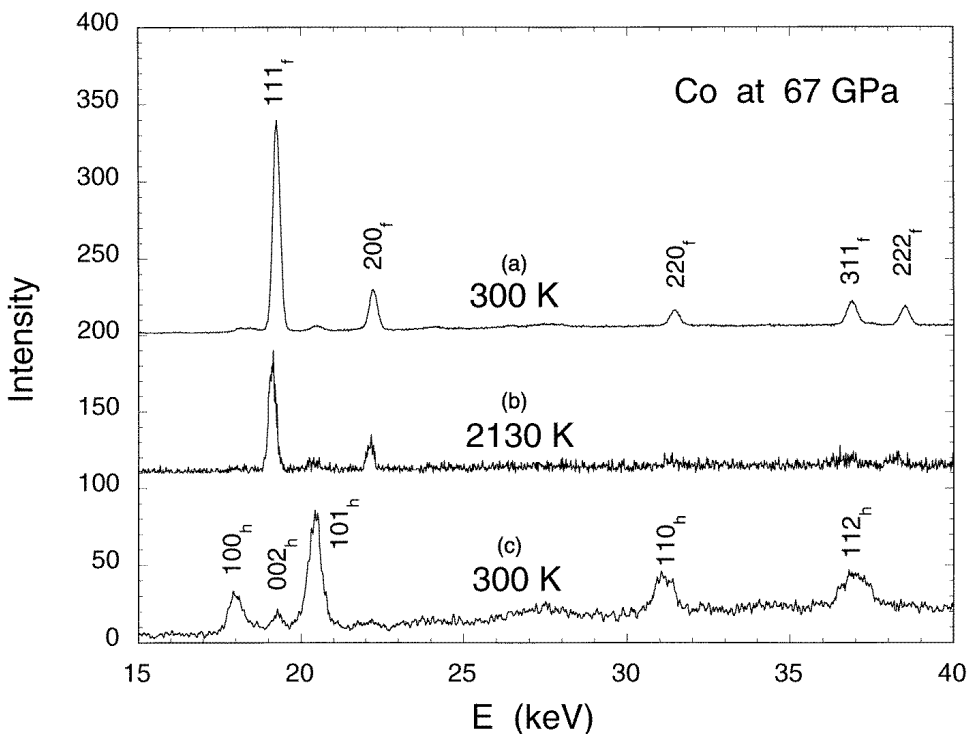


**Figure 2.** X-ray diffraction patterns of laser-heated cobalt at 67 GPa, (a) (300 K) before, (b) (2130 K) during, and (c) (300 K) after heating.

(c) in figure 1, using not all of the reflections but more than ten, indicates a dhcp structure (table 1: denoted as  $\varepsilon'$ -Co). The crystal structure of this  $\varepsilon'$ -phase is a hexagonal structure with an ABAC stacking sequence rather than the ABAB sequence found in  $\varepsilon$ (hcp)-Co. The calculated unit-cell parameters of  $\varepsilon'$ -Co at 34.3 GPa are  $a = 2.421 \text{ \AA}$ ,  $c = 7.722 \text{ \AA}$ , and  $c/a = 3.190$ . The calculated volume,  $59.01 \text{ cm}^3 \text{ mol}^{-1}$ , is nearly identical to that of  $\varepsilon$ -Co,  $58.89 \text{ cm}^3 \text{ mol}^{-1}$ , but is 1% smaller than that of  $\gamma$ -Co,  $59.62 \text{ cm}^3 \text{ mol}^{-1}$ . On the basis of the thermal shifts of the diffraction lines in traces (b) and (c) in figure 1, the thermal volume expansion coefficient of  $\gamma$ -Co is estimated to be  $0.98 \times 10^{-5} \text{ K}^{-1}$  at 34.3 GPa. This result is in good agreement with that for  $\gamma$ -Fe,  $\sim 1.2 \times 10^{-5} \text{ K}^{-1}$  at 34 GPa [17].

The  $\varepsilon'$ -Co phase occurs during the quenching of  $\gamma$ -Co, not during the heating of  $\varepsilon$ -Co, indicating a metastable nature for this phase. A similar dhcp structure has previously been observed for  $\varepsilon'$ -Fe at high pressures [5–7]. The  $c/a$  ratio of  $\varepsilon'$ -Fe is 3.208 at 36 GPa, very close to that of  $\varepsilon'$ -Co. The  $\varepsilon'$ -Fe phase was observed below 40 GPa, whereas,  $\varepsilon'$ -Co is found below 60 GPa as will be shown below. Therefore, these two phases probably represent the same systematics, and we suggest that  $\varepsilon'$ -Fe is also a metastable phase and is different from  $\beta$ -Fe proposed as the phase present at higher pressures and temperatures [7, 8].

The  $\varepsilon'$ -Co phase is found mostly below 60 GPa, whereas  $\gamma$ -Co is found at substantially higher pressures as shown in figures 2 and 3. Furthermore, the  $\gamma$ -Co phase is entirely quenchable at ambient temperature at all of the pressures that we studied. There is almost no indication of  $\varepsilon$ -Co or  $\varepsilon'$ -Co in the quenched sample in trace (c) of figure 2. This result implies that, unlike  $\varepsilon'$ -Co,  $\gamma$ -Co is stable over a wide range of pressures and temperatures,

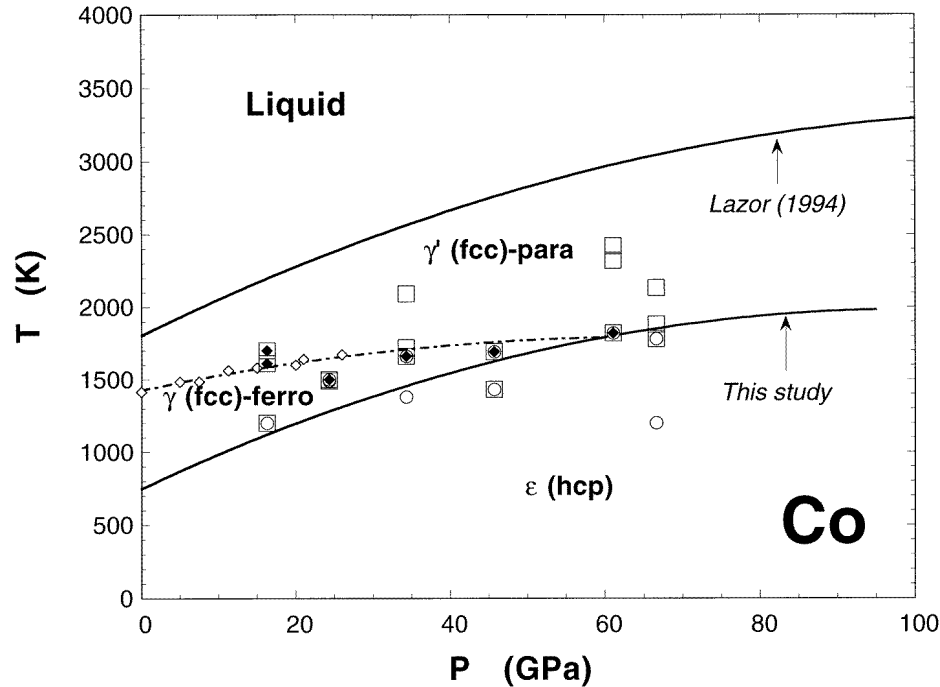


**Figure 3.** The phase diagram of cobalt. The symbols indicate the phases of cobalt as determined by means of *in situ* x-ray diffraction at high pressure and temperature:  $\epsilon$ -Co (open circles) and  $\gamma$ -Co (open squares), and the magnetic transition temperatures (open diamonds [14]). The  $\epsilon/\gamma$ -phase line is drawn below the stability field of  $\gamma$ -Co, and is constrained by the transition temperature at ambient pressure [13]. The  $P, T$  conditions for which  $\epsilon'$ -Co was quenched are also indicated (solid diamonds).

as shown in figure 3.  $\Delta T/\Delta P$  is extremely small for the  $\epsilon/\gamma$ -phase transition,  $\sim 7 \text{ K GPa}^{-1}$ , and, thus, the  $\gamma/\epsilon/\text{liquid}$  triple point should be located substantially above 70 GPa, in sharp contrast with the previous suggestion [14]. This result is, however, in systematic accordance with those for other 3d metals in group VIII. For example, the fcc  $\gamma$ -Fe phase disappears at the  $\gamma/\epsilon/\text{liquid}$  triple point near 40–60 GPa [5, 7, 8], whereas that of Ni is stable even at ambient temperatures [12]. Therefore, the stability of the fcc structure increases with the 3d-electron occupancy from Fe to Co and to Ni.

In figure 3, we reproduce the melting curve and the magnetic transition temperatures below 25 GPa (diamonds) derived from the previous measurements [13, 14]. From this, it becomes immediately evident that  $\epsilon'$ -Co is quenched for the  $P, T$  conditions below the extrapolation of the magnetic transition line between the ferromagnetic  $\gamma$ -phase and the paramagnetic fcc  $\gamma'$ -phase. The  $\gamma/\gamma'$  transition line intersects the  $\epsilon/\gamma$ -phase line at 1800 K and 60 GPa, above which point  $\epsilon'$ -Co is no longer quenchable. This indicates that the  $\epsilon'$ -Co phase appears as a result of magnetism. The fact that the  $\epsilon'$ -phase only appears at relatively low pressures below 60 GPa (40 GPa in the case of  $\epsilon'$ -Fe) supports this conjecture, in view of the fact that the magnetism is rapidly suppressed with increasing pressure.

This interesting behaviour of cobalt motivated us to also study its properties theoretically. We performed magnetic calculations for the fcc, hcp, and dhcp structures of Co up to about 200 GPa, using the full-potential linear muffin-tin orbital (fp-lmto) method [9]. In figure 4

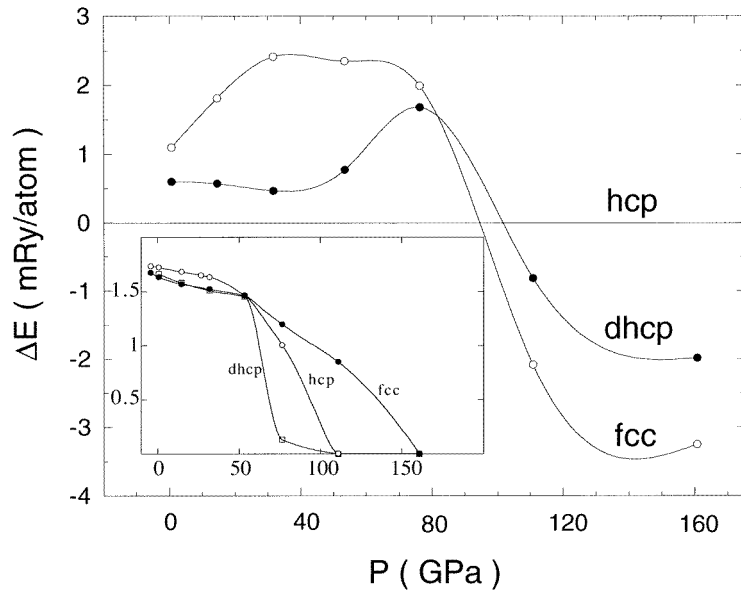


**Figure 4.** The total energies of fcc-Co and dhcp-Co relative to that of hcp-Co. The inset shows the magnetic moment (in Bohr magnetons/atom) as a function of pressure for these three structures.

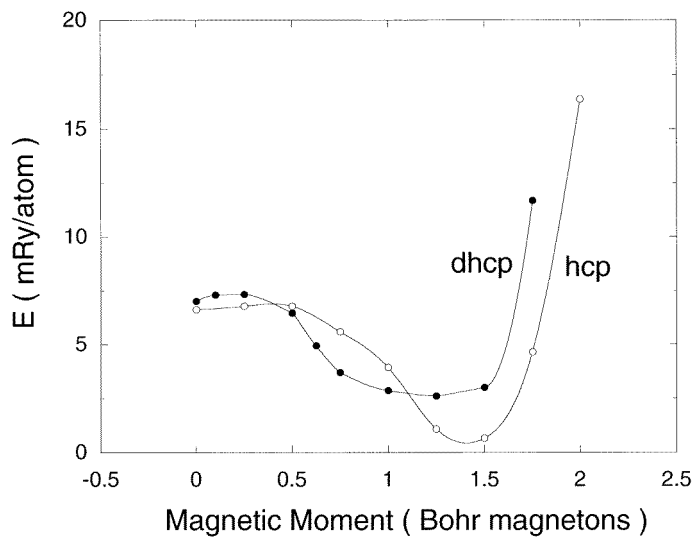


**Figure 5.** The calculated constrained total energies as functions of the spin moment for hcp-Co and dhcp-Co at the volume corresponding to 35 GPa.

we show the calculated total energies of the fcc and dhcp structures with respect to the hcp energy. In the inset, we also plot the magnetic moment as a function of pressure for the fcc, hcp, and dhcp forms of Co. Note that the total energies of the dhcp and hcp structures are indeed very close up to 60 GPa, as are their magnetic moments. At higher pressures

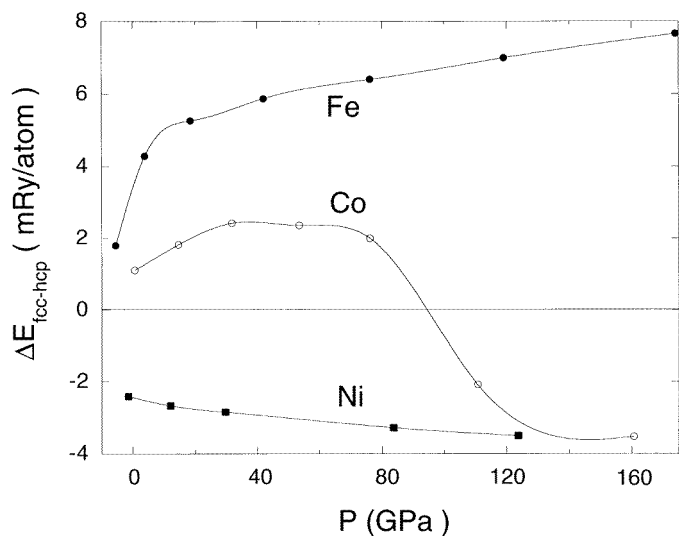


**Figure 6.** The difference in energy between the fcc and hcp phases for Fe, Co, and Ni, as functions of the pressure, as obtained from our fp-lmto calculations.

the magnetism is rapidly suppressed for hcp-Co and dhcp-Co, whereas it persists for fcc-Co up to 150 GPa. It is clear that the magnetic properties of Co are very important for the crystal structure; Co, being in the same column as Rh and Ir, would have been a fcc metal without the formation of a magnetic moment. In fact, at very high pressures, above 100 GPa, where the magnetism is suppressed, we calculate fcc-Co to be more stable than hcp-Co; see figure 4.

At lower pressures and higher temperatures, the crystal structure behaviour of Co is somewhat more complex, and the magnetism plays a key role in stabilizing the crystal structure. Our calculations for high pressure and low temperature show that the total energies for all three structures are very close, particularly for the hcp and dhcp structures. Hence, the relatively small energy contributions arising from temperature effects become very important. It was recently shown, using spin-fluctuation theory [18], that the free energy of fcc-Co intersects that of hcp-Co at 590 K, which is in reasonable agreement with the temperature at which the hcp  $\rightarrow$  fcc transition is observed, about 700 K. In a similar but simplified approach, we study the magnetism of Co using constrained, fixed-spin-moment calculations to compute the total energy as a function of the magnetic spin moment [19]. The results are shown in figure 5. Notice that the dhcp phase has a very broad minimum and that the magnetic moment is considerably more stable than for the hcp phase. This leads to strong spin fluctuations [18] for the dhcp phase with almost no cost in energy, and, in fact, the dhcp energy is lower than the hcp energy for intermediate magnetic moments between 0.5 and 1  $\mu_B$ . Hence, it seems most likely that  $\epsilon'$ -Co is stabilized due to the decrease in magnetism and strong spin fluctuations at high temperatures. The calculated axial ratios for hcp-Co and dhcp-Co are only about 1% larger than the values that we have measured, indicating that we have achieved a good description of Co in our theoretical calculations. Thus, our structural and magnetic calculations for Co support the possibility of a metastable dhcp phase below 60 GPa.

In order to achieve a better understanding of the systematic behaviour of the 3d metals in group VIII, we also computed the stability of the fcc phase versus that of the hcp phase



for Fe, Co, and Ni as a function of pressure up to 150 GPa, as shown in figure 6. Note that the fcc phase becomes progressively more stable going from Fe to Co and finally to Ni, in agreement with our experimental findings. In summary, we have found a new magnetically induced metastable  $\epsilon'$ (dhcp)-Co phase below 60 GPa, and a systematic trend of 3d group VIII elements: the stability of the fcc phase increases with increasing d-electron occupancy in the sequence Fe < Co < Ni. On the basis of this and previous studies [13, 14], we have presented a new phase diagram for Co up to 100 GPa and 3500 K.

We are grateful to J Hu and C Ruddle for experimental assistance at NSLS and SSRL. This work was performed under the auspices of the US Department of Energy at Lawrence Livermore National Laboratory, under contract number W-7405-ENG-48.

## References

- [1] Skriver H L 1985 *Phys. Rev. B* **31** 1909
- [2] Moriarty J 1985 *Phys. Rev. Lett.* **55** 1502
- [3] Duthie J C and Pettifor D G 1977 *Phys. Rev. Lett.* **38** 564
- [4] Söderlind P, Ahuja R, Eriksson O, Wills J M and Johansson B 1994 *Phys. Rev. B* **50** 5918
- [5] Yoo C S, Akella J, Campbell A, Mao H K and Hemley R J 1995 *Science* **270** 1473
- [6] Yoo C S, Söderlind P, Moriarty J A and Campbell A J 1996 *Phys. Lett.* **214A** 65
- [7] Saxena S K, Dubrovinsky L S, Häggkvist P, Cerenius Y, Shen G and Mao H K 1995 *Science* **269** 1703
- [8] Andrault D, Fiquet G, Kunz M, Visocekas F and Häusermann D 1997 *Science* **278** 831
- [9] Söderlind P, Moriarty J A and Wills J M 1996 *Phys. Rev. B* **53** 14 063
- [10] Saxena S K, Dubrovinsky L S, Yoo C S, Akella J, Campbell A J, Mao H K and Hemley R J 1997 *Science* **275** 94
- [11] Anderson O L 1997 *Science* **278** 821
- [12] Young D A 1991 *Phase Diagrams of the Elements* (Livermore, CA: University of California Press)
- [13] Nishizawa T and Ishida K 1983 *Bull. Alloy Phase Diagrams* **4** 387
- [14] Lazor P 1994 *PhD Thesis* Uppsala University
- [15] Saxena S K, Shen G and Lazor P 1994 *Science* **264** 405
- [16] Yoo C S, Cynn H, Campbell A and Hu J-Z 1998 submitted  
Recent double-sided laser-heating results on iron:  
Shen G *et al* 1998 submitted  
have also shown a good agreement with those of reference [5] obtained by using a similar set-up.
- [17] Boehler R, von Barga N and Chopelas A 1990 *J. Geophys. Res.* **95** 21 731
- [18] Uhl M and Kübler J 1996 *Phys. Rev. Lett.* **77** 334
- [19] Schwartz K and Mohn P 1984 *J. Phys. F: Met. Phys.* **14** L129